SPANDIDOS PUBLICATIONS

ONCOLOGY LETTERS 15: 5294-5300, 2018

Contrast-enhanced dynamic and diffusion-weighted magnetic resonance imaging at 3.0 T to assess early-stage nasopharyngeal carcinoma

LIANGPING NI and YING LIU

Department of Radiology, Anhui Medical University Affiliated Anhui Provincial Hospital, Hefei, Anhui 230001, P.R. China

Received September 21, 2017; Accepted January 24, 2018

DOI: 10.3892/ol.2018.7948

Abstract. The present study aimed to assess early-stage nasopharyngeal carcinoma (NPC) with dynamic contrast-enhanced magnetic resonance imaging (DCE-MRI) and diffusion-weighted imaging (DWI) at 3.0 T. A total of 44 patients newly diagnosed with NPC were included in the present study. All patients underwent MR examination at 3.0 T using DCE-MRI and DWI. The volume transfer constant (K^{trans}), flux rate constant between extravascular extracellular space and plasma (K_{ep}), the volume of extravascular extracellular space per unit volume of tissue (V_e) and the apparent diffusion coefficient (ADC) of tumours were investigated. Furthermore, the correlation between clinical stages and ADC value and K^{trans} were analysed. The diagnostic accuracy of K^{trans} and ADC were estimated using receiver operating characteristic curves. NPC stage correlated positively with K^{trans} and negatively with ADC values. Additionally, tumour K^{trans} negatively correlated with ADC value. The sensitivity and accuracy of combined K^{trans} and ADC in distinguishing between stage II and stage III and stage III and IV were higher than the values of either measurement used separately. The present study suggested that K^{trans} and ADC derived from DCE-MRI and DWI may be useful to detect stage early NPC accurately. K^{trans} and ADC in combination were superior than either alone.

Introduction

Among head and neck cancers, nasopharyngeal carcinoma (NPC) has a distinct natural history, aetiology, histopathology, and epidemiology. Male and female incidence of approximately 3:1. Most patients diagnosed with NPC tend to present with stage III or IV disease as a result of its deep location and vague symptoms (1-3). Radiation therapy and chemoradiotherapy are the primary methods of treatment (4), and are administered according to the clinical stage (5), making early diagnosis and staging crucial.

Dynamic contrast-enhanced magnetic resonance imaging (DCE-MRI) has proven useful in characterization of tumour microcirculation and microvascular density. It can delineate the tumour margin from the surrounding tissues (6). DCE-MRI was proved useful in field of differential diagnosis benign and malignant tumours, correlation with tumour grade and stage, early prediction response, and outcome to chemotherapy, radiotherapy and antiangiogenic therapy. Diffusion-weighted imaging (DWI) can indirectly reflect the cell density and microstructure of living tissue (7). Magnetic resonance imaging may be the most powerful and versatile modality in the field of oncology for staging, predicting of treatment response, and identifying disease relapse, particularly in head and neck cancer (8-13). Over-staging and under-staging are the drawbacks of both methods. Various previous studies on bladder and breast cancer demonstrated that the sensitivity and accuracy could be increased by using DCE-MRI and DWI together (14,15). To the best of our knowledge, no study has combined DCE-MRI and DWI together in the diagnosis and staging of early NPC patients. The purpose of the present study was to explore the feasibility and value of DCE-MRI and DWI for early tumour staging in combination using the volume transfer constant (K^{trans}) with DCE-MRI and the apparent diffusion coefficient (ADC) with DWI in NPC patients.

Materials and methods

Clinical data. The study protocol was approved by the Regional Committee for Medical and Health Research Ethics, and all patients signed written informed consent. Forty-six newly diagnosed squamous carcinoma NPC patients in our hospital from December 2014 and October 2015 were included in the study. All underwent DCE-MRI and DWI examinations of the nasopharynx and neck. Two patients were excluded from the study due to a serious motion artefact on pre-treatment MRI exams. Hence, analysis of MRI data was completed on 44 patients (34 males and 10 females, age range, 18-68, mean age, 48 years). All patients' TNM statuses were determined by clinicians according to the International Union Against Cancer (UICC) tumour node metastasis (TNM) staging system: 11 patients were determined to be stage II, 18 were stage III, and 15 were stage IV.

Correspondence to: Professor Ying Liu, Department of Radiology, Anhui Medical University Affiliated Anhui Provincial Hospital, 17 Lujiang Road, Hefei, Anhui 230001, P.R. China
E-mail: lycgz208@yeah.net

Key words: nasopharyngeal neoplasms, magnetic resonance imaging, neoplasm staging

Table I. Dynamic contrast-enhanced magnetic resonance imaging parameters and ADC of 44 patients with nasopharyngeal carcinoma.

	Primary tumours					t-test	
Parameter	II	III	IV	Total	Lateral pterygoid muscle	t	P-value
K^{trans}	1.70±0.36	2.33±0.39	2.61±2.76	2.27±0.49	0.48±0.33	19.93	0.004
K_{ep}	4.4 3±0.91	5.14±1.56	6.12±1.12	5.30±1.43	1.88±1.44	2.94	0.001
V_e	0.61±0.23	0.79±3.45	0.69±2.25	0.71±0.29	0.28±0.15	8.94	0.002
ADC	0.72±0.05	0.68±0.04	0.6 5± 0.05	0.68±0.05	1.25±0.11	27.01	0.001

ADC, apparent diffusion coefficient; K^{trans}, volume transfer constant; K_{ep}, flux rate constant between extravascular extracellular space and plasma; V_e, the volume of extravascular extracellular space per unit volume of tissue.

MRI protocols and procedures. In the present study, we used a 3.0 T whole-body multi-channel phased array scanner system (TrioTim®; Siemens Healthcare, Forchheim, Germany) and a standard head and neck coil. T2-weighted images (T2WI) parameters: Spin-echo (SE) technique: Repetition time 7600 ms, echo time 93 ms, field of view (FOV) 220 mm, flip angle 90˚. DWI were acquired in the axial plane using a spin-echo single-shot echo-planar imaging sequence [TR/TE: 3000/83 ms, section thickness=5 mm, FOV=240 mm, number of signal averages (NSA)=10] with six b-values of 50, 200, 400, 600, 800 and 1,000 sec/mm^2. A set of ADC maps of 10 sections that encompassed the primary tumour in each patient was generated for data analysis.

DCE-MRI protocols. The DCE-MRI used a 3D-T1-fast field echo sequence axial (T1WI-vibe-axial) scan. Pre-contrast T1WI (multi flip angle) were acquired with these parameters: Flip angles=5˚, 10˚ and 15˚; FOV=220 mm; section thickness=5 mm; TR/TE=3.42/1.25 ms; NSA: 1; 26 images per one time phase and one time phase per each flip angle. After the pre-contrast scan, 25 phases of DCE-MRI images were acquired with a 3D T1WI-vibe-axial protocol and the following parameters: Flip angle=10˚ FOV=220 mm, section thickness=5 mm, TR/TE=3.42/1.25 ms; time resolution=6.0 sec. Total scan time was <4 min. Gd-DTPA-BMA was injected at the second time phase of the DCE-MRI protocol with a bolus dose of 0.1 mmol/kg by antecubital vein at a rate of 2.5 ml/sec by a power injector system, followed by a 20-ml saline flush at a rate of 2.5 ml per second. The tumour tissues were compared with the contralateral lateral pterygoid muscle[8].

MRI data analysis. DCE-MRI images were analysed with quantitative analysis software (Omni Kinetics®; GE Healthcare, Beijing, China). Multi flip angle data were uploaded in software for T1 mapping analysis and DCE-MRI data were uploaded for quantitatively permeability and perfusion analysis. Regions of interest (ROIs) for arterial input function (AIF) were set by placing a 3-mm circle over the intracranial internal carotid artery, obtaining a time-concentration curve for permeability quantitative analysis. Extended Tofts Linear two compartmental model was used for permeability analysis, and the volume transfer constant (K^{trans}), the flux rate constant between extravascular extracellular space and plasma (K_{ep}), and the volume of extravascular extracellular space per unit volume of tissue (V_e) of selected slices were calculated by the model as well as the colour map of each parameter. ROIs were placed on the maximum tumour area in the axial plane on the T2-weighted fast spin (T2WI-FS) images to avoid necrosis, capsule and bleeding. We placed 80 mm^2-100 mm^2 ROIs on the opposite lateral pterygoid muscle and measured K^{trans}, K_{ep} and V_e accordingly. We drew the same ROIs on the Siemens workstation to obtain ADC values for comparison with DCE-MRI. All measurements were taken three times and averaged.

Statistical analysis. Data were analysed using commercial software (SPSS 16.0®; IBM, Armonk NY, USA). A P-value of <0.05 was considered statistically significant. Experimental data are presented as arithmetic mean ± standard deviation (SD). The comparison of means used the independent sample t-test. The correlation between K^{trans}, K_{ep}, V_e, ADC and clinical staging were analysed by Pearson rank correlation and linear correlation analysis. The parameters during the period of different clinical were used analysis of variance. ROC curve analysis was applied to assess the sensitivity, specificity and accuracy of K^{trans}, ADC value, or the combination of the two to distinguish between early and advanced stages of NPC.

Results

DCE-MRI parameters and ADC. Mean K^{trans}, K_{ep}, V_e, and ADC values for the tumours and lateral pterygoid muscle are displayed in Table I. NPC presented a higher parameter value than that of normal muscle tissue in the head and neck detected by DCE-MRI technique. The parameters K^{trans}, K_{ep} and V_e of the primary tumours were significantly higher than those of the lateral pterygoid muscle. There were significant differences between tumour and normal internal pterygoid muscle (P<0.05). The ADC values of primary tumours were significantly lower than those of the lateral pterygoid muscle. Boxplots demonstrated the distribution of ADC value and K^{trans} are displayed in Fig. 1. We can see that K^{trans} and ADC showed significant differences between stage II and III, stage II and stage (III and IV). We can see that K^{trans} and ADC values in stage II were both significantly lower and higher, respectively, than those in stage III and IV

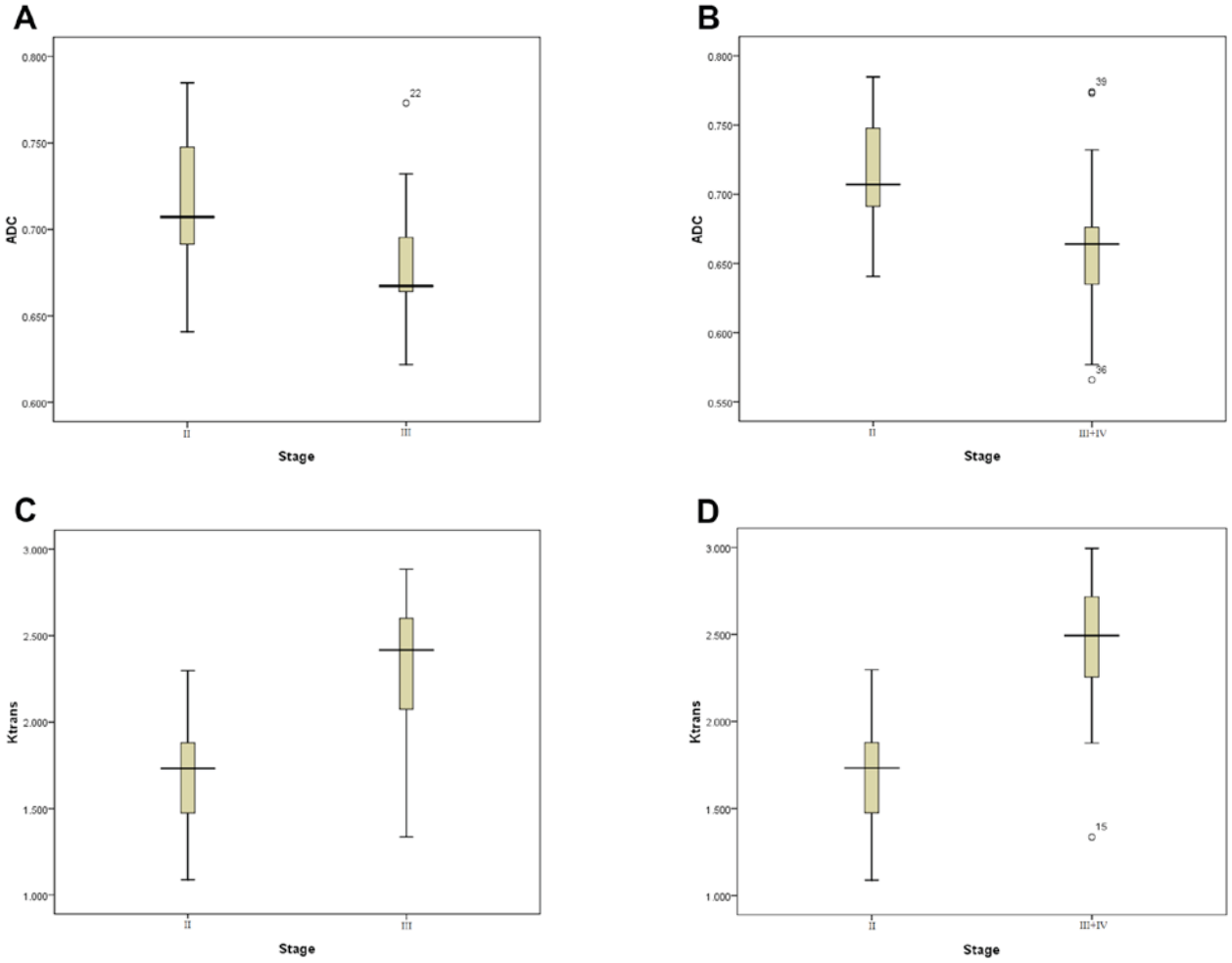

Figure 1. Boxplots demonstrated the distribution of ADC value and K^{trans}. (A) The differences in ADC values between stage II and III (P<0.05). (B) The differences in ADC values between stage II and III+IV (P<0.05). (C) The differences in K^{trans} values between stage II and III (P<0.05). (D) The differences in K^{trans} values between stage II and III+IV (P<0.05).

Table II. Correlation between independent tumour DCE-MRI parameters and ADC values.

Parameter	K_{ep}	V_e	ADC	Stage
K^{trans}	0.42[a]	0.48[a]	-0.34[a]	0.67[a]
K_{ep}		-0.28	-0.21	0.46[a]
V_e			-0.20	0.12
ADC				-0.57[a]

[a]P<0.05, the correlation between the two groups of parameters was statistically significant. DCE-MRI, dynamic contrast-enhanced magnetic resonance imaging; ADC, apparent diffusion coefficient; K^{trans}, volume transfer constant; K_{ep}, flux rate constant between extravascular extracellular space and plasma; V_e, the volume of extravascular extracellular space per unit volume of tissue.

in the Table I. We also determined that the darker the tumour, the greater the K^{trans} value and the higher the stage, as shown in Fig. 2.

Correlations analysis. The relationships between DCE-MRI parameters, ADC and clinical stages are detailed in Table II. Positive correlations were found between clinical stage and K^{trans} (r=0.67, P<0.05) and K_{ep} (r=0.46, P<0.05). ADC showed moderate negative correlation with clinical stage (r=-0.57, P<0.05). V_e revealed no significant correlation with it. In addition, K^{trans} showed negative correlation with ADC value (r=-0.34, P<0.05).

ROC analysis. The sensitivity, specificity, and accuracy obtained by using K^{trans}, ADC and both together to distinguish stage II from stage III and from stage (III and IV) are displayed in Table III. We can see that the sensitivity, specificity, and accuracy obtained by using K^{trans} to distinguish stage II from stage III and from stage (III and IV) are 88.9%; 81.8%; 0.89 and 93.9%; 72.7%; 0.93, respectively. The sensitivity, specificity, and accuracy obtained by using ADC to distinguish stage II from stage III and from stage (III and IV) are 88.9%, 63.6%, 0.79 and 81.8%; 72.7%; 0.83, respectively. The sensitivity, specificity, and accuracy obtained by using K^{trans} and ADC together to distinguish stage II from stage III and from stage (III and IV) are 94.4, 81.8, 0.94 and 97.0%; 81.8%; 0.96, respectively. ROC curve analysis for diagnosing stage II from stage III and stage III+IV by using K^{trans}, ADC and in combination are displayed in Fig. 3. ROC curves show the diagnostic accuracy for early stages based on K^{trans} and ADC values, and

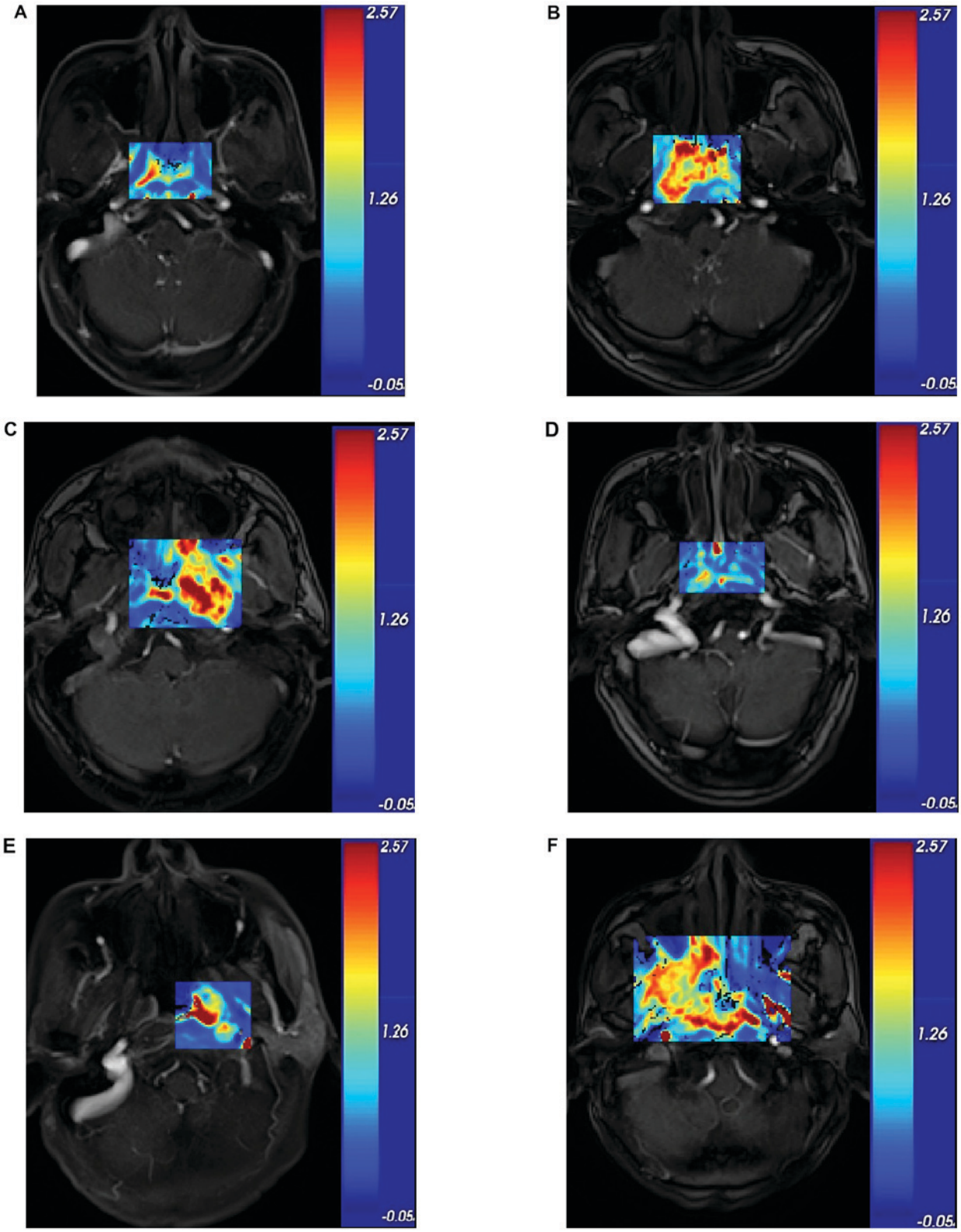

Figure 2. (A-F) Nasopharyngeal K^{trans} axial maps at different stages. (A) stage II patient (A and D) a stage III patient (B and E) a stage IV patient (C and F) Mean K^{trans} values of patients in (A-C) were 1.45, 1.91 and 2.51 min^{-1}, and in (D-F) were 1.35, 1.99, 2.49, respectively. K^{trans} maps of primary tumour presented in (A and D) presented a relatively lower K^{trans} value and lower stage than those in (B and E) and (C and F).

demonstrate excellent AUCs of 0.93 and 0.83, respectively. The diagnostic accuracy of K^{trans} and ADC in differentiation of stage II from stage III were 0.89 and 0.79, respectively. In addition, we found the diagnostic sensitivity and accuracy of K^{trans} and ADC together were higher than either alone.

We determined that K^{trans} and ADC presented significant differences between many early and advanced stages patients. We could see that, with the increase of UICC stage, K^{trans} increased and ADC decreased gradually, respectively. Compared with K^{trans} and ADC, they are more

Table III. Diagnostic sensitivity, specificity and accuracy for early and advanced stages of NPC using K^{trans} and ADC alone or in combination.

	Stage II and III	Stage II and III+IV
Parameter	Sensitivity, Specificity; AUC	Sensitivity, Specificity; AUC
K^{trans}	88.9%; 81.8%; 0.89	93.9%; 72.7%; 0.93
ADC	88.9%; 63.6%; 0.79	81.8%; 72.7%; 0.83
K^{trans} plus ADC	94.4%; 81.8%; 0.94	97.0%; 81.8%; 0.96

AUC, area under the curve; NPC, nasopharyngeal carcinoma; K^{trans}, volume transfer constant; ADC, apparent diffusion coefficient.

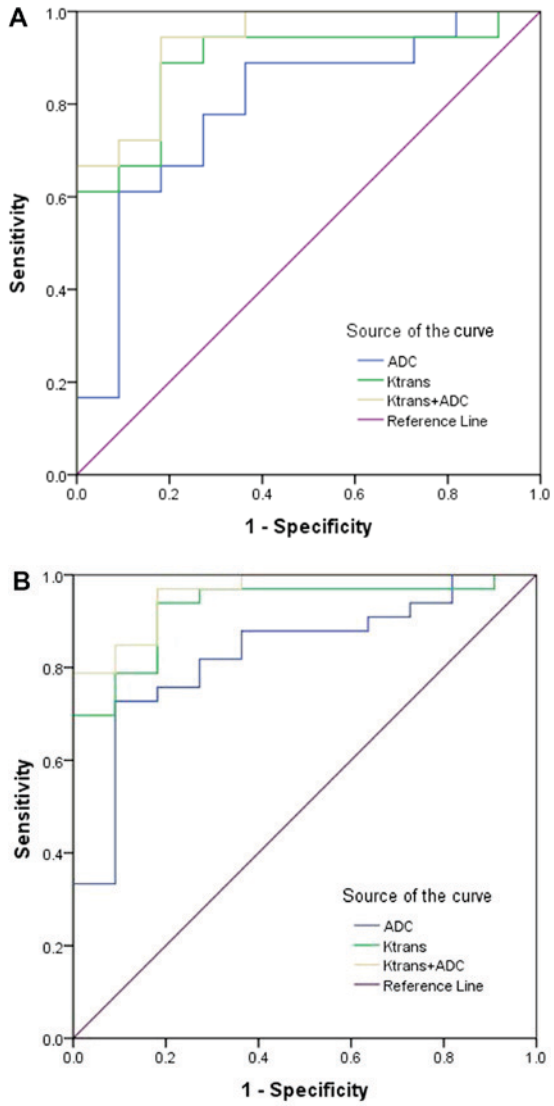

Figure 3. ROC curve analysis for diagnosing stage II from stage III and stage III+IV by using K^{trans}, ADC and in combination. The AUC of K^{trans} and ADC together in the diagnosis of early stage of NPC was 0.94 and 0.96, respectively. (A) stage II vs. stage III. (B) stage II vs. stage III+IV.

valuable and more important parameters in correlating and distinguishing tumour stages.

Discussion

The present study was designed to use K^{trans} and ADC together to improve diagnostic accuracy in the differentiation of early from advanced NPC in newly diagnosed, untreated tumours. A significant positive and negative correlation was found between clinical stage and K^{trans}, and ADC value, respectively. This suggests that K^{trans} and ADC values are significantly associated with characteristics of NPC. In addition, the ROC analysis further showed a good diagnostic performance of K^{trans} and ADC value in assessing early tumour stage.

DWI reflects the random Brownian motion of water molecules within tissues. Malignant tissues show much more diffusion restriction and much lower ADC levels than normal tissues owing to their hypercellularity (16). ADC is a quantitative parameter that can indirectly indicate microvascular circulation, cell membrane integrity, and cell density. It has a high sensitivity and specificity in the diagnosis and staging of tumours (17,18). In the present study, The ADCs of primary tumours were significantly lower than those of muscle. The ADC values in early stage tumours were significantly higher than those in advanced stage tumours ($P<0.05$). A significant correlation of ADC value and clinical stage of NPC was found. The result of the present study is consistent with the previous findings in other tumours (19-21).

Architectural and functional abnormalities of blood vessels are a common feature in tumours (22,23). Estimations of tumour blood volume and permeability obtained with DCE-MRI have been found to correlate with tumour grade, prognosis, and treatment response (24). Previous studies have demonstrated that the increase of vascular endothelial growth factor (VEGF) can induce the proliferation and migration of tumour vascular endothelial cells, and increase the permeability of microvasculature (25). DCE-MRI enables the quantitative assessment of tumour microcirculation properties, including vessel size, distribution and permeability[6]. Tumour tissue is characterised by abundant blood flow, neovascularity, and increased microcirculation permeability, resulting in an increased transfer speed of contrast agent per unit time, such that the K^{trans} values increase with the tumour stage. DCE-MRI can be applied not only to identification and diagnosis of benign and malignant tumours, but also can be used to monitor therapeutic effect and assess prognosis. DCE-MRI is particularly attractive in NPC patients because, comparing to PET or CT, MRI technique is an established and commonly used method for staging and depicting the target volume of NPC patients in China. This pilot clinical study on NPC revealed that there was inhomogeneous microcirculation perfusion inside and outside the tumours. The K^{trans}, K_{ep}, V_e of primary tumours were significantly higher than the values in muscle ($P<0.05$). The Spearman test demonstrated that the K^{trans} of tumours shows positive correlation with clinical stage. These were in concordance with many other studies on other tumours *in vivo*, such as breast cancer (26) and glioma (27).

DWI reflects both diffusion and perfusion. Diffusion is mainly affected by cellularity, presence of oedema, fibrosis, and necrosis of the tissue. The perfusion effect is seen when a b-value of <400 s/mm^2 is used. Malignant tumours have higher perfusion rates than benign tumours (28). Perfusion

can be reflected by DCE-MRI parameters K^{trans}. In the present study, a correlation between tumour K^{trans} and ADC value was observed. The results can be explained because malignant tissues have dense cellularity, large cellular size, and increased micro vessel density and permeability. For these reasons, the accuracy of discriminating early stage from advanced stage NPC using K^{trans} and ADC together was improved.

We also showed that K^{trans} may be a good indicator for early staging in NPC. Therefore, our study demonstrated that both K^{trans} and ADC derived from DCE-MRI and DWI can be helpful tools to discriminate the clinical stage. This not only provides the basis for optimizing the scan sequence, but also provides more MR functional parameters to supplement clinical staging. It can also supplement clinical staging, to further improve the sensitivity and effectiveness of early diagnosis. It can prevent false upstaging and the resulting overtreatment. Guidelines from the National Comprehensive Cancer Network (NCCN) in the US indicate that early treatment of NPC is dominated by radiotherapy alone. Advanced treatment options include concurrent radiotherapy. Simple radiotherapy is not satisfied with the effect of advanced stage (stage III/IV) NPC. Radiotherapy concurrent chemotherapy can well control the local recurrence of tumour lesion and distant metastasis, which can significantly improve the survival time of patients. Early NPC patients with satisfactory results of radiotherapy alone, generally do not need synchronous chemotherapy, can largely help patients reduce the side effects of chemotherapy drugs and radioactive injury, etc, can well improve the quality life of patients. Therefore, the early diagnosis of NPC and accurate clinical stage of its treatment plan and the prognosis of patients plays a crucial role.

However, the present study has several limitations, including the small sample size and the lack of comparison between different types of NPC. Further investigation on more cases may improve the statistical power. DCE-MRI postprocessing needs high temporal resolution to improve the accuracy of the maps, but the slice coverage of a DCE-MRI sequence is limited. In addition, there are still some challenges to overcome when using DCE-MRI and DWI on children, elderly, or other special groups who could not endure a long examination time. Hence, the DCE-MRI and DWI technique may need further development.

In conclusion, K^{trans} derived from DCE-MRI and ADC derived from DWI have a good potential to accurately stage early NPC. The two parameters used together offer the best accuracy.

References

1. Lee AW, Lin JC and Ng WT: Current management of nasopharyngeal cancer. Semin Radiat Oncol 22: 233-244, 2012.
2. Boscolo-Rizzo P, Tirelli G, Mantovani M, Baggio V, Lupato V, Spinato G, Gava A and Da Mosto MC: Non-endemic locoregional advanced nasopharyngeal carcinoma: Long-term outcome after induction plus concurrent chemoradiotherapy in everyday clinical practice. Eur Arch Otorhinolaryngol 272: 3491-3498, 2015.
3. Chen Y, Liu X, Zheng D, Xu L, Hong L, Xu Y and Pan J: Diffusion-weighted magnetic resonance imaging for early response assessment of chemoradiotherapy in patients with nasopharyngeal carcinoma. Magn Reson Imaging 32: 630-637, 2014.
4. Yi JL, Gao L, Huang XD, Li SY, Luo JW, Cai WM, Xiao JP and Xu GZ: Nasopharyngeal carcinoma treated by radical radiotherapy alone: Ten-year experience of a single institution. Int J Radiat Oncol Biol Phys 65: 161-168, 2006.
5. Spratt DE and Lee N: Current and emerging treatment options for nasopharyngeal number carcinoma. Onco Targets Ther 5: 297-308, 2012.
6. Türkbey B, Thomasson D, Pang Y, Bernardo M and Choyke PL: The role of dynamic contrast-enhanced MRI in cancer diagnosis and treatment. Diagn Interv Radiol 16: 186-192, 2010.
7. Pan J, Zang L, Zhang Y, Hong J, Yao Y, Zou C, Zhang L and Chen Y: Early changes in apparent diffusion coefficients predict radiosensitivity of human nasopharyngeal carcinoma xenografts. Laryngoscope 122: 839-843, 2012.
8. Huang B, Wong CS, Whitcher B, Kwong DL, Lai V, Chan Q and Khong PL: Dynamic contrast enhanced magnetic resonance imaging for characterising nasopharyngeal carcinoma: Comparison of semiquantitative and quantitative parameters and correlation with tumour stage. Eur Radiol 23: 1495-1502, 2013.
9. Zheng D, Chen Y, Chen Y, Xu L, Chen W, Yao Y, Du Z, Deng X and Chan Q: Dynamic contrast-enhanced MRI of nasopharyngeal carcinoma: A preliminary study of the correlations between quantitative parameters and clinical stage. J Magn Reson Imaging 39: 940-948, 2014.
10. Abdel Razek AA and Kamal E: Nasopharyngeal carcinoma: Correlation of apparent diffusion coefficient value with prognostic parameters. Radiol Med 118: 534-539, 2013.
11. Vandecaveye V, Dirix P, De Keyzer F, de Beeck KO, Vander Poorten V, Roebben I, Nuyts S and Hermans R: Predictive value of diffusion-weighted magnetic resonance imaging during chemoradiotherapy for head and neck squamous cell carcinoma. Eur Radiol 20: 1703-1714, 2010.
12. Kim S, Loevner LA, Quon H, Kilger A, Sherman E, Weinstein G, Chalian A and Poptani H: Prediction of response to chemoradiation therapy in squamous cell carcinomas of the head and neck using dynamic contrast-enhanced MR imaging. AJNR Am J Neuroradiol 31: 262-268, 2010.
13. Powell C, Schmidt M, Borri M, Koh DM, Partridge M, Riddell A, Cook G, Bhide SA, Nutting CM, Harrington KJ and Newbold KL: Changes in functional imaging parameters following induction chemotherapy have important implications for individualised patient-based treatment regimens for advanced head and neck cancer. Radiother Oncol 106: 112-117, 2013.
14. Zhou G, Chen X, Zhang J, Zhu J, Zong G and Wang Z: Contrast-enhanced dynamic and diffusion-weighted MR imaging at 3.0T to assess aggressiveness of bladder cancer. Eur J Radiol 83: 2013-2018, 2014.
15. Kul S, Cansu A, Alhan E, Dinc H, Gunes G and Reis A: Contribution of diffusion weighted imaging to dynamic contrast-enhanced MRI in the characterization of breast tumors. AJR Am J Roentgenol 196: 210-217, 2011.
16. Hong J, Yao Y, Zhang Y, Tang T, Zhang H, Bao D, Chen Y and Pan J: Value of magnetic resonance diffusion-weighted imaging for the prediction of radio sensitivity in nasopharyngeal carcinoma. Otolaryngol Head Neck Surg 149: 707-713, 2013.
17. Fong D, Bhatia KS, Yeung D and King AD: Diagnostic accuracy of diffusion weighted MR imaging for nasopharyngeal carcinoma, head and neck lymphoma and squamous cell carcinoma at the primary site. Oral Oncol 46: 603-606, 2010.
18. Li H, Liu XW, Geng ZJ, Wang DL and Xie CM: Diffusion-weighted imaging to differentiate metastatic from non-metastatic retropharyngeal lymph nodes in nasopharyngeal carcinoma. Dentomaxillofac Radiol 44: 20140126, 2015.
19. Kobayashi S, Koga F, Kajino K, Yoshita S, Ishii C, Tanaka H, Saito K, Masuda H, Fujii Y, Yamada T and Kihara K: Apparent diffusion coefficient value reflects invasive and proliferative potential of bladder cancer. J Magn Reson Imaging 39: 172-178, 2014.
20. Langer DL, van der Kwast TH, Evans AJ, Plotkin A, Trachtenberg J, Wilson BC and Haider MA: Prostate tissue composition and MR measurements: Investigating the relationships between ADC, T2, K^{trans}, v_e and corresponding histologic features. Radiology 255: 485-494, 2010.
21. Lee J, Choi SH, Kim JH, Sohn CH, Lee S and Jeong J: Glioma grading using apparent diffusion coefficient map: Application of histogram analysis based on automatic segmentation. NMR Biomed 27: 1046-1052, 2014.
22. Guo AC, Cummings TJ, Dash RC and Provenzale JM: Lymphomas and high-grade astrocytomas: Comparison of water diffusibility and histologic characteristics. Radiology 224: 177-183, 2002.

23. Yao WW, Zhang H, Ding B, Fu T, Jia H, Pang L, Song L, Xu W, Song Q, Chen K and Pan Z: Rectal Cancer: 3D dynamic contrast-enhanced MRI; correlation with microvascular density and clinicopathological features. Radiol Med 116: 366-374, 2011.
24. Law M, Oh S, Babb JS, Wang E, Inglese M, Zagzag D, Knopp EA and Johnson G: Low-grade gliomas: Dynamic susceptibility-weighted contrast-enhanced perfusion MR imaging prediction of patient clinical response. Radiology 238: 658-667, 2006.
25. Möbius C, Freire J, Becker I, Feith M, Brücher BL, Hennig M, Siewert JR and Stein HJ: VEGF-C expression in squamous cell carcinoma and adenocarcinoma of the esophagus. World J Surg 31: 1768-1772, 2007.
26. El Khouli RH, Macura KJ, Kamel IR, Jacobs MA and Bluemke DA: 3-T dynamic contrast-enhanced MRI of the breast: Pharmacokinetic parameters versus conventional kinetic curve analysis. AJR Am J Roentgenol 197: 1498-1505, 2011.
27. Arevalo-Perez J, Peck KK, Young RJ, Holodny AI, Karimi S and Lyo JK: Dynamic contrast-enhanced perfusion MRI and diffusion-weighted imaging in grading of gliomas. J Neuroimaging 25: 792-798, 2015.
28. Woodhams R, Matsunaga K, Kan S, Hata H, Ozaki M, Iwabuchi K, Kuranami M, Watanabe M and Hayakawa K: ADC mapping of benign and malignant breast tumors. Magn Reson Med Sci 4: 35-42, 2005.